

Research Article

Structures, Morphological Control, and Antibacterial Performance of Ag/TiO₂ Micro-Nanocomposite Materials

Muhammad Akhsin Muflikhun ¹, Alvin Y. Chua ² and Gil N. C. Santos³

¹Department of Mechanical and Industrial Engineering, Faculty of Engineering, Gadjah Mada University, Jl. Grafika No. 2, Yogyakarta 55281, Indonesia

²Department of Mechanical Engineering, De La Salle University, 2401 Taft Avenue, Manila, Philippines

³Department of Physics, De La Salle University, 2401 Taft Avenue, Manila, Philippines

Correspondence should be addressed to Muhammad Akhsin Muflikhun; akhsin.muflikhun@ugm.ac.id

Received 14 February 2019; Revised 1 April 2019; Accepted 9 April 2019; Published 7 May 2019

Guest Editor: Joanna Rydz

Copyright © 2019 Muhammad Akhsin Muflikhun et al. This is an open access article distributed under the Creative Commons Attribution License, which permits unrestricted use, distribution, and reproduction in any medium, provided the original work is properly cited.

Structures, morphological control, and antibacterial activity of silver-titanium dioxide (Ag/TiO₂) micro-nanocomposite materials against *Staphylococcus aureus* are investigated in this study. Horizontal vapor phase growth (HVPG) technique was used to synthesize the Ag/TiO₂ micro-nanomaterials, with parameters of growth temperature and baking time. The materials were characterized by using scanning electron microscopy (SEM), energy dispersive X-ray (EDX) spectroscopy, and atomic force microscope (AFM). The result indicated that the HVPG technique is able to synthesize Ag/TiO₂ with many shapes in micro- and nanoscale such as nanoparticles, nanorods, triangular nanomaterials, and nanotubes. The results showed that the shape of micro- and nanocomposites material could be arranged by adjusting the parameters. The results revealed that the nanorods structure were obtained at 1000°C growth temperature and that 8 hours of baking time was ideal for antibacterial application. Treating the *S. aureus* stock with Ag/TiO₂ nanocomposites is able to reduce bacterial growth with a significant result.

1. Introduction

Recent forays into novel developments of medical research have involved nanomaterials as useful tools to combat cancer or bacteria, viruses, and other microbial pathogens [1–4]. Nanomaterials based on silver, titanium dioxide, carbon, and graphene have been studied for food packaging process, especially for medical applications such as anti-pathogenic activity or tissue regeneration [5–8]. There are eight main applications for nanotechnology in medicine: pathogen detection, protein detection, DNA structure penetration, tissue engineering, tumor eradication, pathogenic cell or molecule eradication, magnetic resonance imaging, and phagokinetic studies [9–11].

Synthetic silver or Ag/TiO₂ nanomaterials have been developed and successfully manufactured by several methods due to the wide applications that are found tremendously in different fields. The synthetic methods include

chemical reduction [12], chemical vapor deposition [13], electrochemical [14], green synthesis [15], HVPG [16–18], microwave [19], photochemical [20], radiation [21], and sonochemical [22].

In the case of synthesized silver-titanium nanocomposite, the research of this material applied in medical and health applications had attracted many researchers. Table 1 shows the use of silver-titanium dioxide nanocomposite material for antibacterial applications that has been performed in the previous study.

The previous study shows nanocomposite materials successfully synthesized by using HVPG technique. This technique offers certain advantages as follows: a large amount of nanocomposites material can be fabricated from the limited amount of powder-form source material, the synthesis occurred at the vacuum condition that minimizes contaminants, and by adjusting baking time and growth temperature, variations of the nanostructures can be

TABLE 1: Previous study of Ag/Ti nanomaterials.

Source	Purpose of the study	Results
Martinez-Gutierrez et al. [23]	To compare the antibacterial properties of Ag, Ti, and Ag/Ti	Silver with size 20 nm to 25 nm was the most effective against bacteria.
Liga et al. [24]	To determine the relationship between silver concentration and its effectiveness to eradicate bacteria	The higher the proportion of silver in the silver-titanium nanoparticles, the more effective the nanomaterials against bacteria.
Motlagh et al. [25]	To determine the relationship between the size of nanomaterials and its effectiveness to eradicate bacteria	Ag/Ti nanomaterials with the size between 10 nm and 30 nm show excellent results against bacteria.
Song et al. [26]	To investigate the advanced applications of Ag/Ti nanomaterials	Ag/Ti nanomaterials have excellent mechanical properties as coating materials that can be implemented in implant technology.
Yang et al. [1]	To investigate the Ag/Ti nanomaterials against bacteria	List of bacteria that can be treated by using Ag/Ti nanomaterials: <i>Staphylococcus aureus</i> , <i>Bacillus subtilis</i> , <i>Candida albicans</i> , <i>Pseudomonas aeruginosa</i> , <i>Escherichia coli</i> , and <i>Klebsiella pneumoniae</i> .
Mei et al. [27]	To investigate the Ag/Ti nanomaterials related to the dental field	Encompassing anodization method was used to synthesize titanium, and plasma immersion ion implantation method was used to synthesize silver that can produce nanotubes and can be effective against bacteria on dental implant cases.
Cao et al. [4]	To explain the application of Ag/Ti nanomaterials that is compatible with osteoblasts	The Ag/Ti nanomaterials were capable and compatible with osteoblasts synthesized using the plasma immersion ion implantation method to produce nanomaterials with size 25 nm.
Wang et al. [28]	To investigate the applications of Ag/Ti nanomaterials synthesized by using hydrothermal and irradiation methods	Ag/Ti nanobelts can be coated into paper sheet applied in food and medical technology.
Besinis et al. [8]	To investigate the best nanomaterials that are used against dental bacterial	Comparison between silver, titanium, and silver-titanium nanomaterials against <i>Streptococcus mutans</i> . The results show that silver is the best material against bacteria.

produced. Moreover, statistics analysis of synthesis nanomaterials by using the HVPG technique reported that it was capable of creating nanomaterials with various shapes such as nanoparticles, nanorods, triangular nanomaterials, and nanotubes. [17, 18, 29, 30]. Table 2 shows the previous work that has been done by researchers regarding synthesized various nanomaterials by using the HVPG technique.

The goal of this study is to investigate the structures and morphological behavior of Ag/TiO₂ micro-nanocomposites materials synthesized by using the HVPG technique. The study also evaluated the antibacterial effect of Ag/TiO₂ nanocomposite materials against the gram-positive bacterium *S. aureus*, one of the species that is commonly infectious to humans [35–37] with bacterial colonies quantified through the pour plate technique. The micro-nanostructures synthesized from the HVPG technique were evaluated by using SEM and EDX to determine the shape of the Ag/TiO₂ micro-nanocomposite. The AFM is used to determine the 3D surface roughness of the nanocomposite to explain the geometrical effect of nanocomposite that can eradicate bacteria. The antibacterial testing was conducted by comparing 2 different types of tubes with and without Ag/TiO₂. By synthesizing the above material with HVPG technique and investigating with SEM, EDX, AFM, and pour plate technique, it is a step forward in the development of manufacturing of silver-

titanium dioxide nanomaterials for antibacterial purposes with a simple, noncontaminant technique, which shapes a variety of nanomaterials.

2. Materials and Methods

The starting material was a mixture of 17.5 mg silver (Ag) powder from Aldrich Corporation and 17.5 mg titanium dioxide (TiO₂) powder from Degussa P25. JEOL JSM-5310 scanning electron microscopy (SEM) was used to image and measure the synthesized nanomaterials found at all three zones of the tube. Energy dispersive X-ray spectroscopy (EDX) was used to determine the composition of the material in terms of silver or titanium dioxide. The 3D surface roughness of nanocomposite material was characterized by using Park System XE-100 atomic force microscopy (AFM).

The silica quartz tubes with an outer diameter of 11 mm and an inner diameter of 8.5 mm are used as the vessels for synthesis. The quartz tubes containing silver and titanium dioxide powder then were evacuated using the thermionic high vacuum system to create vacuum conditions with a pressure of approximately 10⁻⁶ Torr and then sealed. This effectively sterilizes the tubes and removes possible contaminating substances.

Figure 1 shows the nanocomposite materials after sealing and then placed half inside the furnaces and divided into 3

TABLE 2: Previous study of nanomaterials synthesized via HVPG technique.

Source	Materials name	Result
Briones et al. [18]	Tin dioxide (SnO_2)	Nanostructures formed into nanowires and used for gas sensing applications
Shimizu et al. [29]	Skewered phthalocyanine $[\text{Fe}^{\text{III}}(\text{Pc})(\text{SCN})]_n$	Source material can be converted into crystalline nanostructures (nanorods) with $2\ \mu\text{m}$ width and $10\ \mu\text{m}$ length
Quitaneq and Santos [31]	Cadmium Selenide (CdSe)	Nanocrystallites with size 100 nm to 400 nm
Reyes and Santos [32]	Tin dioxide (SnO_2)	Nanostructures formed into nanowires, nanorods, nanoparticles, and nanobelts
Buot and Santos [33]	Carbon-silver (C/Ag)	Micro-nanocomposites with size from 100 nm to $1.5\ \mu\text{m}$ for battery electrode applications
Muflikhun et al. [34]	Silver-graphene (Ag/Ge)	Micro-nanocomposite materials with size from 100 nm to $2\ \mu\text{m}$

zones. The tubes were placed horizontally, with variable baking times of 4, 6, and 8 hours and variable temperatures growth of 800°C , 1000°C , and 1200°C . The tubes were only halfway inserted into the furnace, creating a temperature gradient between the hotter region inside the furnace and the cooler region outside the furnace. Figure 2 schematically depicts the vaporization of the source material located in the furnace and subsequent deposition outside the furnace.

To quantify bacterial colonies, McFarland standard 0.5 was used, with serial dilutions to dilution factors 10^{-3} to 10^{-6} . About 1.5×10^{-8} CFU/mL of inoculum of test organism, which is *S. aureus*, is spread onto the agar plate. The plate was placed on the inoculated plates and then incubated at 37°C for 16–24 hours. The pour plate technique was used to grow the colonies under three different setups: negative control of only the bacterial suspension and two setups with the nanocomposites of 17.5 gram Ag and 17.5 gram TiO_2 [38–40].

A vortex mixer was used to homogenize the *S. aureus* suspension with the Ag/TiO_2 nanocomposites. This was inoculated into Petri dishes and incubated at room temperature for 18 hours before colony counting. Figure 3 shows a flowchart of the experiment conducted in the study.

3. Results and Discussion

3.1. Material Characterization via SEM and EDX. SEM revealed the external morphology of the nanocomposites, while EDX determines its relative composition. Figure 4 shows the SEM image of Ag/TiO_2 material before it was mixed. The results show that most of the materials are macro in size and in bulk form. In this study, the nanomaterials deposited at different zones of the quartz tube were separately investigated by using SEM.

Figure 5 shows the SEM images of the as-prepared hybrid nanocomposite materials Ag/TiO_2 with a baking time of 4 hours. As shown, the materials are not fully transformed to its nanosized form and visible in zone 3 and partially shown in zone 2 both at 800°C of growth temperature. The results indicate that the baking time is not enough to evaporate silver and titanium dioxide macro-materials to nanoscale especially at 800°C growth temperature. Some amount of Ag and TiO_2 bulk materials source

material still had not changed into nanomaterials. In contrast, nanomaterials exhibit in zone 2 and zone 3 at 1000°C and 1200°C growth temperature. The nanoparticle size ranges from 700 to 1416 nm.

Figure 6 shows that the majority of silver nanomaterials were detected after Ag/TiO_2 evaporated in zone 1, zone 2, and zone 3. The particles were exhibited on the inner surface of the silica tubes. It also indicates that the majority of the Ag/TiO_2 deposit appeared at zone 2 of the tube. EDX spectroscopy in Figure 7 shows the majority of the material consisting silver exhibits in zone 2 of the tube at 1200°C growth temperature and 6 hours baking time. This phenomenon occurred due to inadequate growth temperature for the evaporation of TiO_2 .

Figure 8 shows the SEM images of the Ag/TiO_2 nanocomposite materials. The results indicate that the majority of materials appear to be nanoparticles and nanorods. The diameter of the nanocomposites varies and has different shapes with different baking time. The results show that the smallest diameter of nanocomposites in all combinations occurred at 8 hours baking time and 1000°C growth temperature with a range of 361 nm–382 nm. In this combination, especially at zone 2, the silver nanorods are extended with sharp end and covered by nanocotton-like titanium dioxide.

The average diameters of the micro- and nanocomposites concerning the parameters of the study which are baking time and growth temperature are shown in Table 3. The material measurements based on SEM image and EDX results were evaluated from 3 different points as shown in Figure 9(a). The measurement method was performed by manual calculation. The results show the diameter of nanocomposites can be predicted statistically [17]. The results show that the smallest average diameter of micro-nanocomposite occurred at the 1000°C growth temperature and 8 hours baking time.

Size, shape, and surface of the nanocomposites are the several critical aspects in determining their interaction behavior with cells. The study proved that the smaller the nanocomposites size, the higher the antimicrobial efficiency of the nanocomposites due to their direct interaction with the interface of the bacteria (membrane). Furthermore, the shape of the nanocomposites could directly influence the

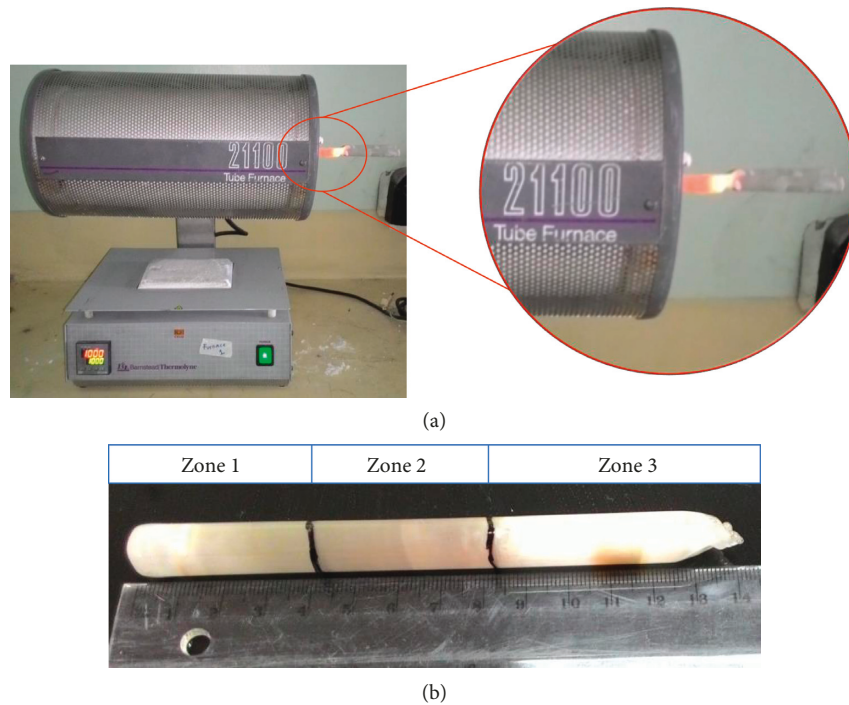


FIGURE 1: (a) Horizontal furnace. (b) Quartz tube after baking.

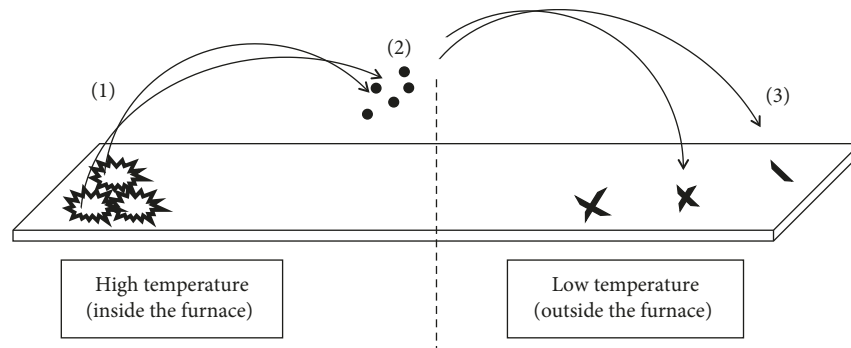


FIGURE 2: HVPG schematics: (1) source macromaterials placed at the end of the tube inside the furnace, (2) the materials changing to particles, and (3) the nanocomposite materials depositing on the parts of the tube outside the furnace.

available contact area required to facilitate the interactions of nanocomposites with the bacterial membrane [41]. Silver nanoplates and silver nanorods showed higher antimicrobial activity towards bacteria compared to other silver nano-shapes [10]. The silver nanorods were capable of inhibiting all viable *S. aureus* cells within 4 hours by using 5 ppm silver nanorods solution and 3.5 hours by using 10 pp solution, respectively [42]. Moreover, based on Table 3 and images from SEM, 8 hours of baking time followed by 1000°C growth temperature could be an effective way to achieve high antimicrobial efficacy. The results show the nanocomposites diameter is from 300 nm to 600 nm with the majority of nanomaterials form as nanorods.

Figure 9 shows Ag/TiO₂ nanorods with diameters around 300 nm to 400 nm (Figure 9(a)). Other forms of the synthesized nanocomposite include strand-like or

cotton-like structures with bigger diameters that addressed to Ag/TiO₂ micro-nanocomposites (Figure 9(b)). EDX analysis (Figure 9(c)) revealed appropriate amounts of Ag, Ti, and O in the nanocomposites along with Si likely from the quartz tube and Au from the coating material.

Figure 9 shows the typical Ag/TiO₂ nanorods synthesized via HVPG technique. It is shown that silver nanomaterials are grown with the titanium dioxide covered on the surface. By using EDX spectroscopy, the nanorods come from silver nanomaterials, and cotton-like nanomaterials are from titanium dioxide nanomaterials. Furthermore, the results show that combination of silver and titanium dioxide can be fabricated with a controllable diameter as explained in the previous study by Muflikhun et al. [17]. To ensure Ag/TiO₂ is capable of eradicating bacteria, the antibacterial test

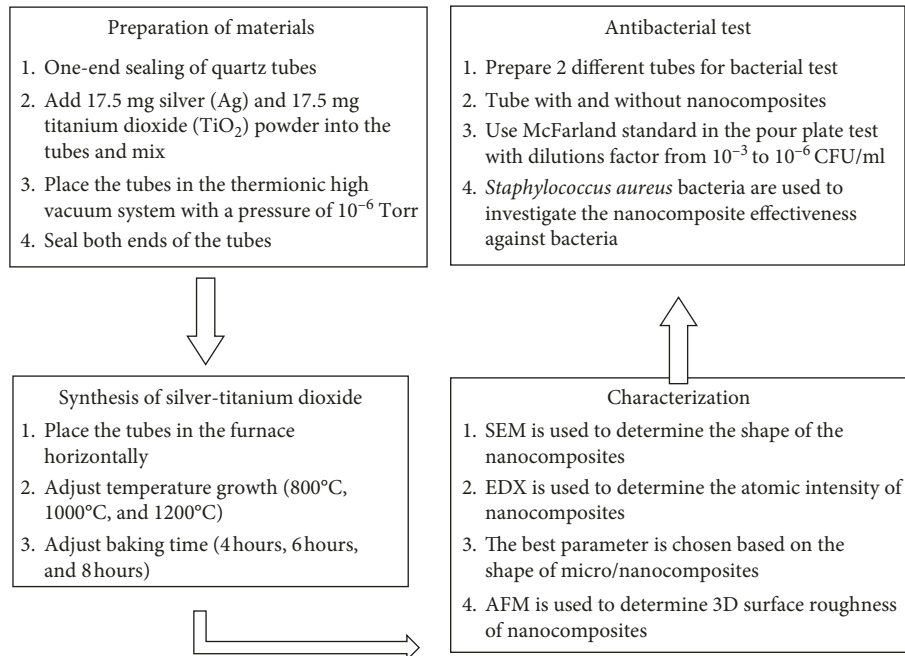


FIGURE 3: A detailed flowchart of the study.

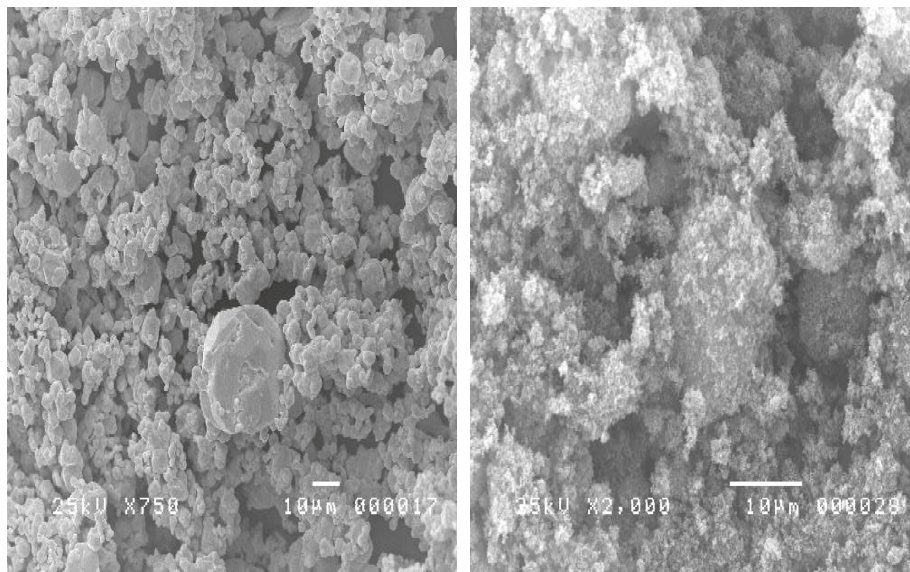


FIGURE 4: Silver material (a) and titanium dioxide material (b).

was conducted by using a combination tube with 8 hours baking time and 1000°C growth temperature.

3.2. Investigation of Antibacterial Property. The antibacterial property of the Ag/TiO₂ nanocomposites were tested against *S. aureus* colonies. The standard analysis was conducted through the 0.5 McFarland standard (approximately 1.5×10^8 CFU/mL). Serial dilution was performed with dilution factors from 10^{-3} to 10^{-6} . Figures 10 and 11 show the colonies grown at dilution factors 10^{-5} and 10^{-6} , with and without the nanocomposites.

Figures 10 and 11 show that treatment with the Ag/TiO₂ nanocomposites resulted in curbing the growth of *S. aureus* colonies. The result and images are presented as the significant capability of Ag/TiO₂ nanocomposite to eradicate the *S. aureus* in terms of the amount of *S. aureus* with the nanocomposites. The antibacterial efficacy of the nanocomposite treatment is computed, and the complete data collected from counting bacterial colony growth in the different setups are compiled in Table 4.

Table 4 shows the bacterial test by using the Ag/TiO₂ nanocomposite material (nanorods). The results show the

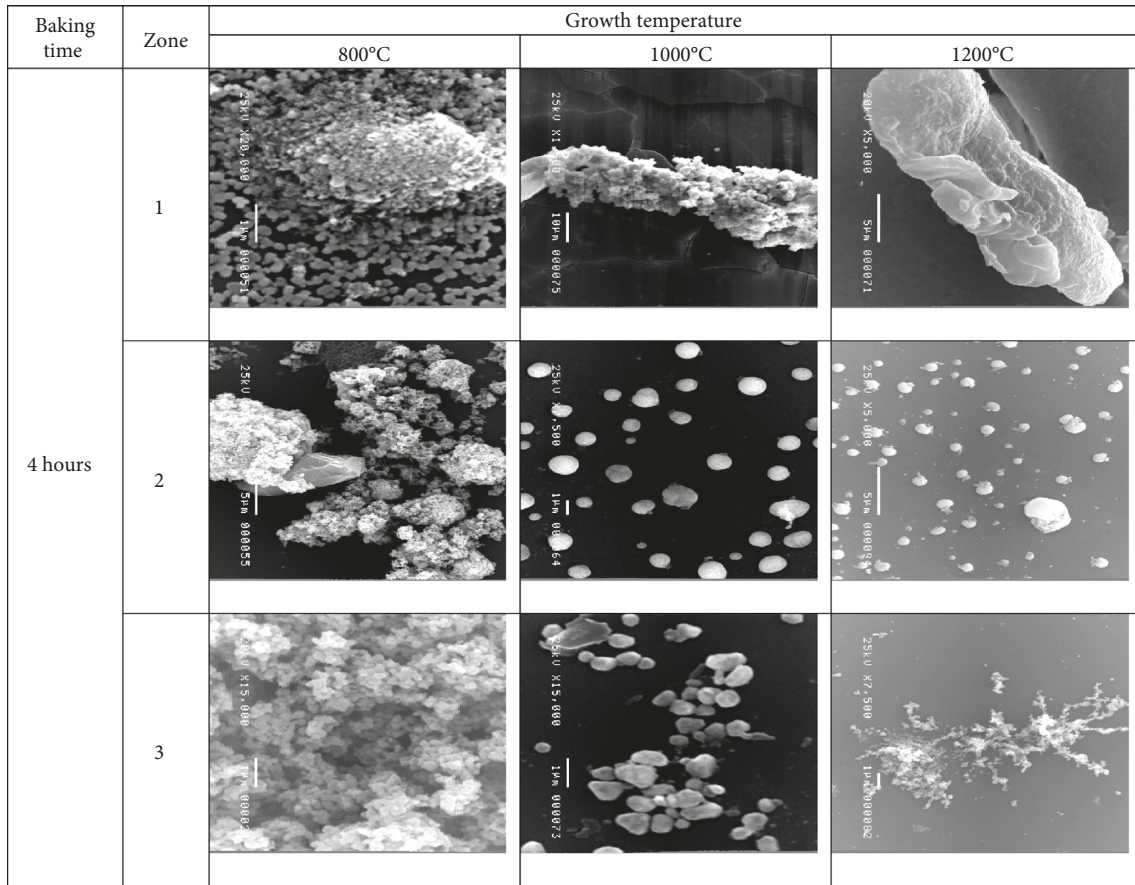


FIGURE 5: SEM image after 4 hours of baking time.

nanocomposite materials are successfully capable of reducing bacterial growth with approximately 75% efficiency. It can be noted that the test is based on the dilution factor by using a 0.5 McFarland standard. The solution that contains bacterial colony was placed inside the tube that consists of nanomaterials. The tube that did not contain nanomaterials was used as the control plate. The tubes were rotated and shaken for around 5 minutes by using a Vertex machine to mix the bacterial colony with nanocomposite materials. The bacterial colony attached Ag/TiO₂ nanorods when the rotation occurred. Since there is no standard for shaking and rotating the tubes by using the Vertex machine, the efficiency of the treatment can be improved by increasing the amount of nanocomposite material and the rotating time. Presumably, the more the nanorods formed and the longer the shaking time, the faster the bacteria eradication.

3.3. Nanocomposite Growth Mechanism. The synthesis of nanomaterials by using the HVPG technique is based on the thermal method where the material is changed at different stages as shown in Figure 12. The conversion depends on the temperature wherein, at low temperature, the material becomes solid. At high temperature, the material becomes liquid (at melting point) and gas (at boiling point) before it condenses in lower temperature and becomes solid again. In

the case of Ag/TiO₂ nanocomposite material, the shape of the nanocomposite depends on the growth temperature and baking time. The higher temperature will fasten the material conversion from liquid to gas and move from zone 1 (inside the furnace) to zone 2 and zone 3. Longer baking time will speed up the material deposit mostly in the bigger size (micro and nano) at zone 2 and zone 3, and lower baking time will create the smaller size of nanocomposite materials in zone 2 and zone 3.

3.4. Antibacterial Mechanism. Modification of silver nanomaterials with specific shape combined with titanium dioxide nanomaterials gives significant results in effectiveness against *S. aureus*. To understand the mechanism of how nanorods can eradicate the bacteria, some relevant papers discussed the nanomaterials contacted to bacteria should be considered. The previous studies conducted by Hajipour et al. [35] and Salata [9] show that nanomaterials have higher efficiency in eradicating bacteria. Bacteria are a robust organism that its cell wall is designed to provide strength and can protect its cell from osmotic rupture and physical damages. As a result, there are two common ways to eradicate bacteria, by the toxicity mechanism and by breaking the membrane of bacteria by the mechanical process. By toxicity, nanoparticles can attach to the membrane of bacteria by

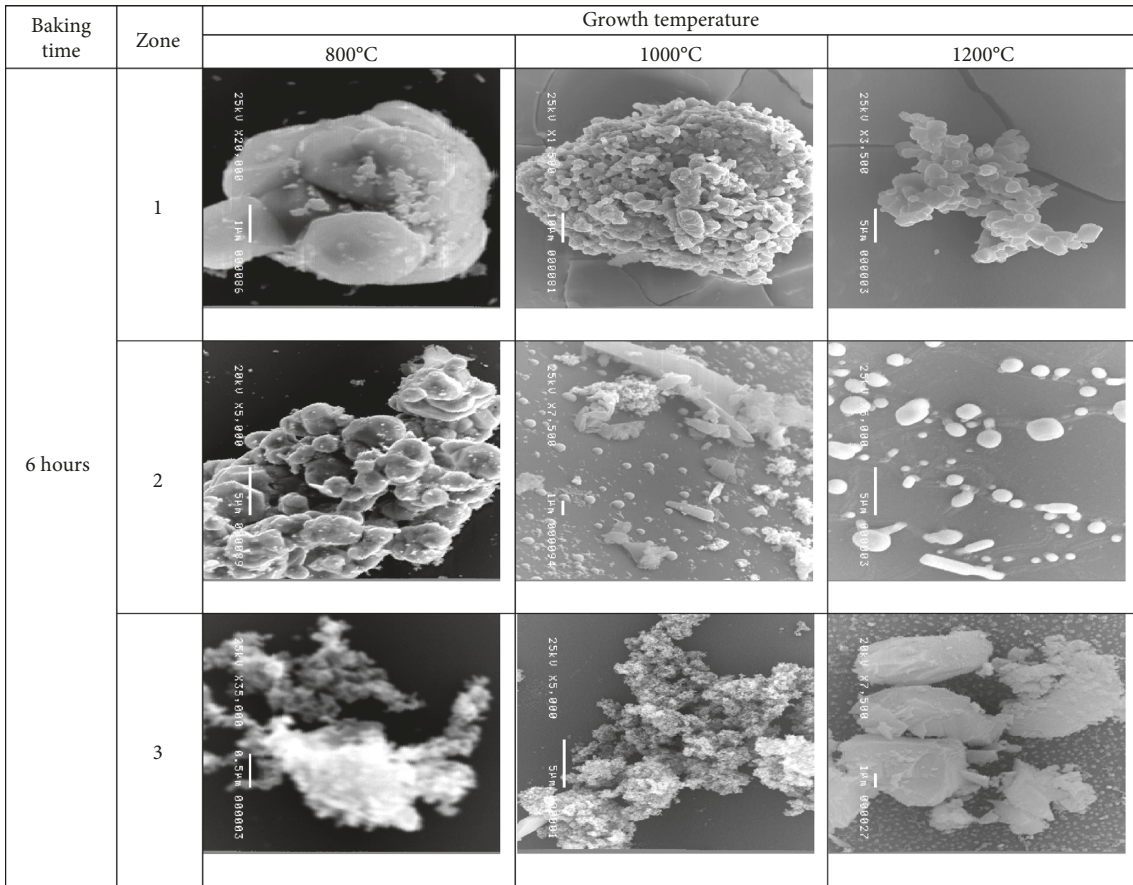


FIGURE 6: SEM image from 6 hours of baking time.

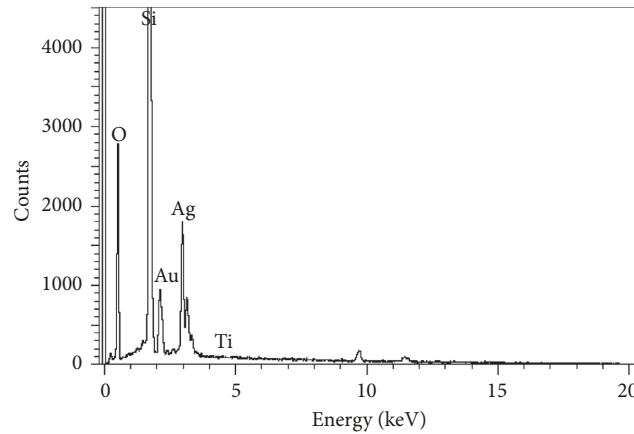


FIGURE 7: EDX result from zone 2 of the sample at 1200°C growth temperature and 6 hours baking time.

electrostatic interaction and disturb the integrity of it. For example, TiO₂ nanomaterials are toxic to the bacterial only under ultraviolet (UV) illumination. The effectiveness of TiO₂ under UV light was able to eradicate the bacteria in 1 hour. The mechanism of TiO₂ to eradicate the bacteria can increase peroxidation of the polyunsaturated phospholipid component in the lipid membrane. This condition can disturb cell respiration. The Ag nanomaterials can eradicate bacteria by

penetrating their membrane and increasing the toxicity in the presence of external magnetic field, electrostatic interaction, and physical damage of the bacteria [9, 35].

In this study, the nanocomposite materials are reported with the unique ability of Ag/TiO₂ to eradicate bacteria caused by physical damage due to its shape. The present study shows that silver nanomaterials can be fabricated with a different shape depending on the baking time and growth temperature. Among the various shapes of nanomaterials,

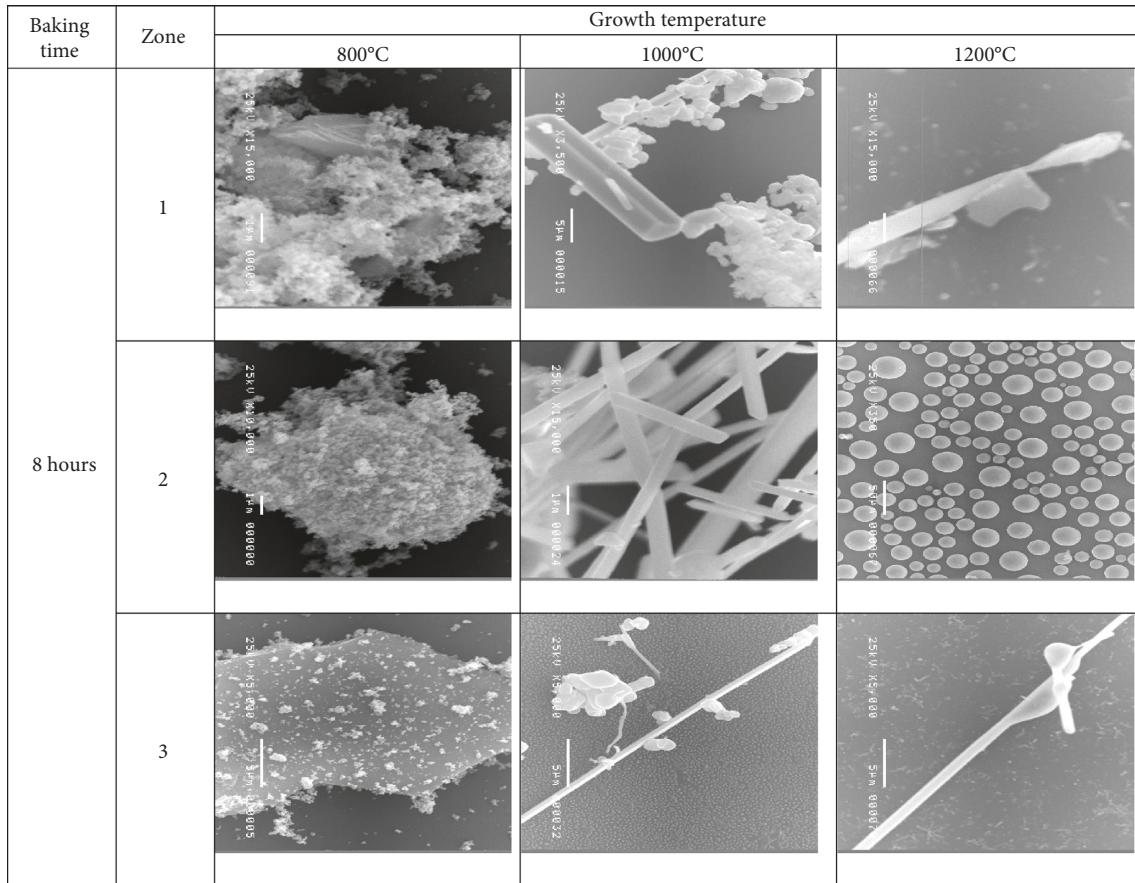


FIGURE 8: SEM image from 8 hours of baking time.

TABLE 3: Average diameters of micro-nanocomposite synthesized at each zone for all parameter settings.

Baking time	Zone	Growth temperature		
		800°C	1000°C	1200°C
4 hours	1	0.177 μm	19.133 μm	7.547 μm
	2	7.010 μm	1.416 μm	0.863 μm
	3	1.604 μm	0.707 μm	1.066 μm
6 hours	1	0.313 μm	2.689 μm	2.012 μm
	2	3.501 μm	0.477 μm	9.406 μm
	3	0.904 μm	1.233 μm	0.541 μm
8 hours	1	3.226 μm	0.651 μm	0.617 μm
	2	0.832 μm	0.382 μm	8.354 μm
	3	1.212 μm	0.562 μm	0.706 μm

nanorods are the one candidate that can be used to eradicate bacteria by using its geometry. The shape of nanorods was sharp at the top of it, and this shape can break the membrane of the bacteria. The *S. aureus* membrane size has been investigated by Touhami et al. [43], and Lee et al. [44] show that the bacterial cell wall and plasma membrane are around 10–20 nm thickness. By using the nanorods that have sharp end on the top of it, the bacterial membrane can be broken, and it caused physical damage to the bacteria. The schematic of bacterial eradication (not to scale) and AFM test are shown in Figure 13.

4. Conclusion

The HVPG technique was successfully used to synthesize silver-titanium dioxide micro-nanocomposites, with the desired optimal nanorods structures fabricated at 1000°C for 8 hours. The SEM and EDX analyses were used to characterize the material. The pour plate technique was used to grow *S. aureus* colonies to determine the antibacterial activity.

The SEM and EDX analyses revealed that the micro- and nanoparticles, nanorods, triangular nanomaterials, and nanotubes were successfully produced in high proportions. Antibacterial treatment with the Ag/TiO₂ nanocomposites was able to reduce bacterial growth by approximately 75%. This result indicated that the bacteria were successfully eradicated with Ag/TiO₂ nanocomposites. In general, the effect of adding Ag/TiO₂ will give more significant effect on the performance of nanocomposite materials to eradicate *S. aureus*. The result is strongly dependent on the growth temperature and baking time to produce and increase the amount of nanorods that have been proven more effective to eradicate bacteria. Furthermore, the study was capable of controlling the structures and morphology of micro- and nanomaterials based on growth temperature and baking time. In the future, the effect of Ag/TiO₂ nanocomposites

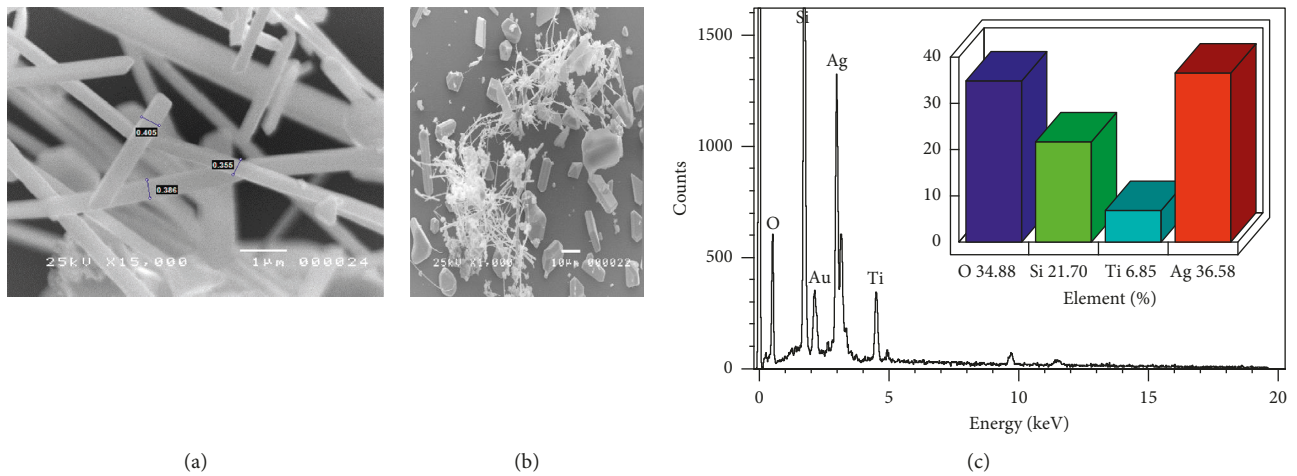


FIGURE 9: (a) Ag/TiO₂ nanorods grown at 1000°C for 8 hours; (b) other spots in the same tube shows different results, including cotton-like growths. (c) EDX results of Ag/TiO₂ from (a) [17].

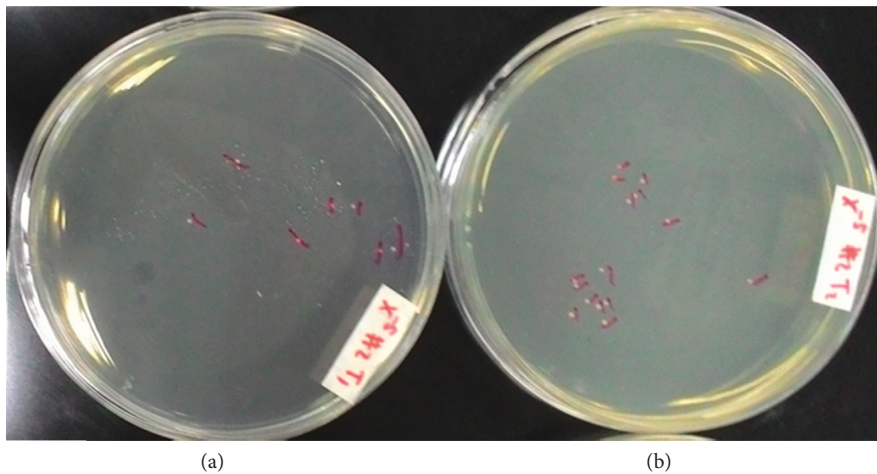


FIGURE 10: *S. aureus* colonies diluted 10⁻⁵ grown (a) with and (b) without the Ag/TiO₂ nanocomposites.

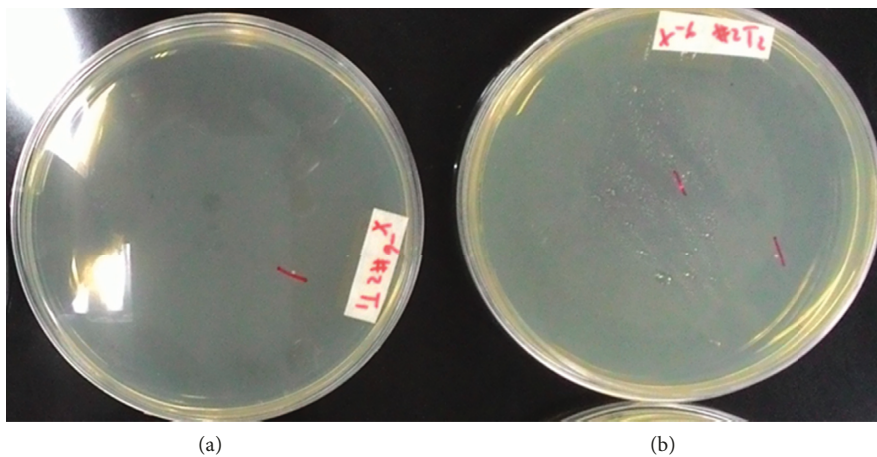


FIGURE 11: *S. aureus* colonies diluted 10⁻⁶ grown (a) with and (b) without the Ag/TiO₂ nanocomposites.

TABLE 4: The number of bacterial colonies for each setup, at each dilution factor.

Tube	Materials	Dilution factor (number of colonies)														
		10^{-3}				10^{-4}				10^{-5}				10^{-6}		
		#1	#2	#3	Ave.	#1	#2	#3	Ave.	#1	#2	#3	Ave.	#1	#2	Ave.
1	Zero (control tube)	>100	>100	>100	>100	>100	>100	>100	>100	12	15	14	14	2	2	2
2	50% Ag, 50% TiO ₂	>100	>100	>100	>100	>100	>100	>100	>100	6	7	7	6.3	1	0	0.5
3	50% Ag, 50% TiO ₂	>100	>100	>100	>100	>100	>100	>100	>100	10	12	10	10,7	0	1	0.5

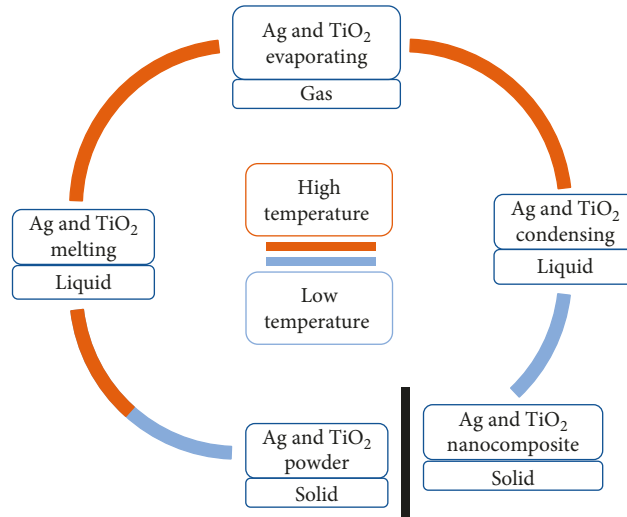
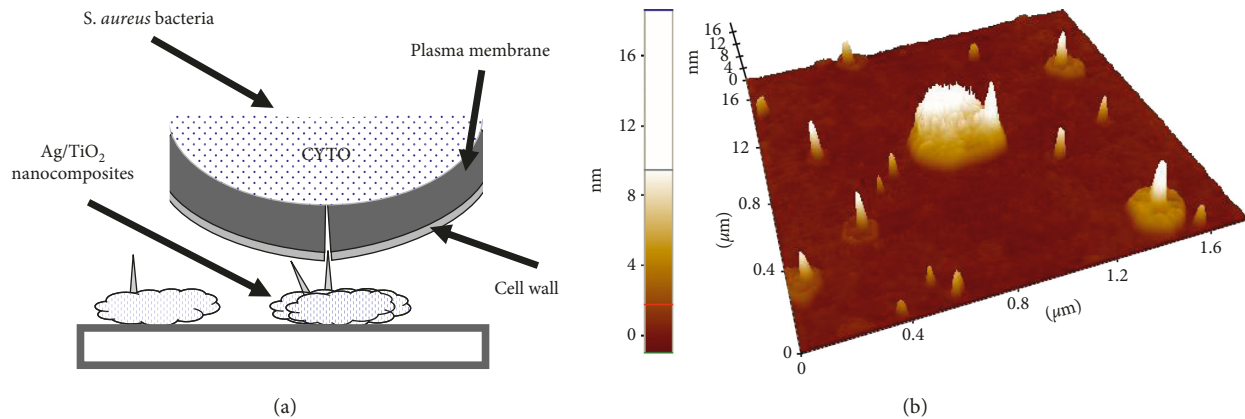


FIGURE 12: Material conversion.

FIGURE 13: (a) Schematic of nanocomposites eradicating bacteria (not to scale) and (b) AFM image of Ag/TiO₂ nanocomposite materials.

will be studied for their antibacterial property with different types of bacteria and will be tested against fungi as well as bacteria.

Data Availability

No data were used to support this study.

Conflicts of Interest

The authors declare that there are no conflicts of interest in this study.

Acknowledgments

The study was supported by the Solid State Physics Lab, Mechanical Engineering Department of De La Salle University, and AUN SEED NET Project JICA Funding. The authors would also thank Siwat Manomaisantiphap for reviewing the manuscript and Gwen Castillon for assisting during the experiment.

References

- [1] F.-C. Yang, K.-H. Wu, J.-W. Huang, D.-N. Horng, C.-F. Liang, and M.-K. Hu, "Preparation and characterization

- of functional fabrics from bamboo charcoal/silver and titanium dioxide/silver composite powders and evaluation of their antibacterial efficacy,” *Materials Science and Engineering: C*, vol. 32, no. 5, pp. 1062–1067, 2012.
- [2] F. Baghbani-arani, R. Movagharnia, A. Sharifian, S. Salehi, S. A. S. Shandiz, and S. Shandiz, “Photo-catalytic, antibacterial, and anti-cancer properties of phyto-mediated synthesis of silver nanoparticles from artemisia tournefortiana Rchb extract,” *Journal of Photochemistry and Photobiology B: Biology*, vol. 173, pp. 640–649, 2017.
 - [3] S. J. Lee, M. Heo, D. Lee et al., “Preparation and characterization of antibacterial orthodontic resin containing silver nanoparticles,” *Applied Surface Science*, vol. 432, pp. 317–323, 2018.
 - [4] H. Cao, X. Liu, F. Meng, and P. K. Chu, “Biological actions of silver nanoparticles embedded in titanium controlled by micro-galvanic effects,” *Biomaterials*, vol. 32, no. 3, pp. 693–705, 2011.
 - [5] S. Sarkar, A. D. Jana, S. K. Samanta, and G. Mostafa, “Facile synthesis of silver nano particles with highly efficient antimicrobial property,” *Polyhedron*, vol. 26, no. 15, pp. 4419–4426, 2007.
 - [6] M. B. Faiz, R. Amal, C. P. Marquis et al., “Nanosilver and the microbiological activity of the particulate solids versus the leached soluble silver,” *Nanotoxicology*, vol. 12, no. 3, pp. 263–273, 2018.
 - [7] A. Llorens, E. Lloret, P. A. Picouet, R. Trbojevich, and A. Fernandez, “Metallic-based micro and nanocomposites in food contact materials and active food packaging,” *Trends in Food Science & Technology*, vol. 24, no. 1, pp. 19–29, 2012.
 - [8] A. Besinis, T. De Peralta, and R. D. Handy, “The antibacterial effects of silver, titanium dioxide and silica dioxide nanoparticles compared to the dental disinfectant chlorhexidine on *Streptococcus mutans* using a suite of bioassays,” *Nanotoxicology*, vol. 8, no. 1, pp. 1–16, 2014.
 - [9] O. Salata, “Applications of nanoparticles in biology and medicine,” *Journal of Nanobiotechnology*, vol. 2, no. 1, p. 3, 2004.
 - [10] K. Zheng, M. I. Setyawati, D. T. Leong, and J. Xie, “Antimicrobial silver nanomaterials,” *Coordination Chemistry Reviews*, vol. 357, pp. 1–17, 2018.
 - [11] N. K. Rajendran, S. S. D. Kumar, N. N. Houreld, and H. Abrahamse, “A review on nanoparticle based treatment for wound healing,” *Journal of Drug Delivery Science and Technology*, vol. 44, pp. 421–430, 2018.
 - [12] Z. Khan, S. A. Al-Thabaiti, A. Y. Obaid, and A. O. Al-Youbi, “Preparation and characterization of silver nanoparticles by chemical reduction method,” *Colloids and Surfaces B: Biointerfaces*, vol. 82, no. 2, pp. 513–517, 2011.
 - [13] O. Beier, A. Pfuch, K. Horn, J. Weisser, M. Schnabelrauch, and A. Schimanski, “Low temperature deposition of antibacterially active silicon oxide layers containing silver nanoparticles, prepared by atmospheric pressure plasma chemical vapor deposition,” *Plasma Processes and Polymers*, vol. 10, no. 1, pp. 77–87, 2013.
 - [14] G. R. Nasretidinova, R. R. Fazleeva, R. K. Mukhitova et al., “Electrochemical mediated synthesis of silver nanoparticles in solution,” *Russian Journal of Electrochemistry*, vol. 51, no. 11, pp. 1029–1040, 2015.
 - [15] S. Patra, S. Mukherjee, A. K. Barui, A. Ganguly, B. Sreedhar, and C. R. Patra, “Green synthesis, characterization of gold and silver nanoparticles and their potential application for cancer therapeutics,” *Materials Science and Engineering: C*, vol. 53, pp. 298–309, 2015.
 - [16] M. A. Muflikhun, G. N. Santos, and A. Y. Chua, “Synthesis and characterization of silver-titanium nanocomposite via horizontal vapor phase growth (HVPG) technique,” in *Proceedings of the DLSU Research Congress*, pp. 1–5, Manila, Philippines, March 2015.
 - [17] M. A. Muflikhun, A. Y. Chua, and G. N. C. Santos, “Statistical design analysis of silver-titanium dioxide nanocomposite materials synthesized via horizontal vapor Phase growth (HVPG),” *Key Engineering Materials*, vol. 735, pp. 210–214, 2017.
 - [18] J. C. Briones, G. Castillon, M. P. Delmo, and G. N. C. Santos, “Magnetic-field-enhanced morphology of tin oxide nanomaterials for gas sensing applications,” *Journal of Nanomaterials*, vol. 2017, Article ID 4396723, 11 pages, 2017.
 - [19] X. Hong, J. Wen, X. Xiong, and Y. Hu, “Shape effect on the antibacterial activity of silver nanoparticles synthesized via a microwave-assisted method,” *Environmental Science and Pollution Research*, vol. 23, no. 5, pp. 4489–4497, 2016.
 - [20] J. S. Gabriel, V. A. M. Gonzaga, A. L. Poli, and C. C. Schmitt, “Photochemical synthesis of silver nanoparticles on chitosans/montmorillonite nanocomposite films and antibacterial activity,” *Carbohydrate Polymers*, vol. 171, pp. 202–210, 2017.
 - [21] Y. Liu, S. Chen, L. Zhong, and G. Wu, “Preparation of high-stable silver nanoparticle dispersion by using sodium alginate as a stabilizer under gamma radiation,” *Radiation Physics and Chemistry*, vol. 78, no. 4, pp. 251–255, 2009.
 - [22] R. A. Salkar, P. Jeevanandam, S. T. Aruna, Y. Koltypin, and A. Gedanken, “The sonochemical preparation of amorphous silver nanoparticles,” *Journal of Materials Chemistry*, vol. 9, no. 6, pp. 1333–1335, 1999.
 - [23] F. Martinez-Gutierrez, P. L. Olive, A. Banuelos et al., “Synthesis, characterization, and evaluation of antimicrobial and cytotoxic effect of silver and titanium nanoparticles,” *Nanomedicine Nanotechnology, Biology and Medicine*, vol. 6, no. 5, pp. 681–688, 2010.
 - [24] M. V. Liga, E. L. Bryant, V. L. Colvin, and Q. Li, “Virus inactivation by silver doped titanium dioxide nanoparticles for drinking water treatment,” *Water Research*, vol. 45, no. 2, pp. 535–544, 2011.
 - [25] A. L. Motlagh, S. Bastani, and M. M. Hashemi, “Investigation of synergistic effect of nano sized Ag/TiO₂ particles on antibacterial, physical and mechanical properties of UV-curable clear coatings by experimental design,” *Progress in Organic Coatings*, vol. 77, no. 2, pp. 502–511, 2014.
 - [26] D.-H. Song, S.-H. Uhm, S.-B. Lee, J.-G. Han, and K.-N. Kim, “Antimicrobial silver-containing titanium oxide nanocomposite coatings by a reactive magnetron sputtering,” *Thin Solid Films*, vol. 519, no. 20, pp. 7079–7085, 2011.
 - [27] S. Mei, H. Wang, W. Wang et al., “Antibacterial effects and biocompatibility of titanium surfaces with graded silver incorporation in titania nanotubes,” *Biomaterials*, vol. 35, no. 14, pp. 4255–4265, 2014.
 - [28] J. Wang, W. Liu, H. Li et al., “Preparation of cellulose fiber-TiO₂ nanobelt-silver nanoparticle hierarchically structured hybrid paper and its photocatalytic and antibacterial properties,” *Chemical Engineering Journal*, vol. 228, pp. 272–280, 2013.
 - [29] E. Shimizu, G. N. Santos, and D. E. Yu, “Nanocrystalline axially bridged iron phthalocyanine polymeric conductor: (μ -thiocyanato)(phthalocyaninato)iron(III),” *Journal of Nanotechnology*, vol. 2016, Article ID 5175462, 7 pages, 2016.
 - [30] W. V. Espulgar and G. N. C. Santos, “Antimicrobial silver nanomaterials synthesized by HVPG technique,”

- International Journal of Scientific & Engineering Research*, vol. 2, no. 8, pp. 8–11, 2011.
- [31] A. C. Quitaneg and G. N. C. Santos, “Cadmium selenide quantum dots synthesized by HVPC growth technique for sensing copper ion concentrations,” *International Journal of Scientific & Engineering Research*, vol. 2, no. 12, pp. 1–4, 2011.
- [32] R. D. L. Reyes and G. N. C. Santos, “Growth mechanism of SnO₂ nanomaterials derived from backscattered electron image and EDX observations,” *International Journal of Scientific & Engineering Research*, vol. 2, no. 12, pp. 1–4, 2011.
- [33] R. M. N. Buot and G. N. C. Santos, “Synthesis and characterization of C-Ag nanomaterials for battery electrode application,” *International Journal of Scientific & Engineering Research*, vol. 3, no. 2, pp. 1–3, 2012.
- [34] M. A. Muflikhun, G. B. Castillon, G. N. C. Santos, and A. Y. Chua, “Micro and nano silver-graphene composite manufacturing via horizontal vapor Phase growth (HVPG) technique,” *Materials Science Forum*, vol. 901, pp. 3–7, 2017.
- [35] M. J. Hajipour, K. M. Fromm, A. Akbar Ashkarran et al., “Antibacterial properties of nanoparticles,” *Trends in Biotechnology*, vol. 30, no. 10, pp. 499–511, 2012.
- [36] W. G. I. U. Rathnayake, H. Ismail, A. Baharin, A. G. N. D. Darsanasiri, and S. Rajapakse, “Synthesis and characterization of nano silver based natural rubber latex foam for imparting antibacterial and anti-fungal properties,” *Polymer Testing*, vol. 31, no. 5, pp. 586–592, 2012.
- [37] S. K. Ray, D. Dhakal, C. Regmi, T. Yamaguchi, and S. W. Lee, “Inactivation of *Staphylococcus aureus* in visible light by morphology tuned α -NiMoO₄,” *Journal of Photochemistry and Photobiology A: Chemistry*, vol. 350, pp. 59–68, 2018.
- [38] E. Goldman and E. G. L. H. Green, *Practical Handbook of Microbiology*, CRC Press, Boca Raton, FL, USA, 1990.
- [39] D. Burdass, J. Grainger, and J. Hurst, “Part 1: the basics an introduction to microbiology, aseptic technique and safety,” in *Basic Practical Microbiology A Manual*, pp. 1–40, Society for General Microbiology (SGM), London, UK, 2006.
- [40] M. A. Muflikhun, M. C. Frommelt, M. Farman, A. Y. Chua, and G. N. C. Santos, “Structures, mechanical properties and antibacterial activity of Ag/TiO₂ nanocomposite materials synthesized via HVPG technique for coating application,” *Heliyon*, vol. 5, no. 4, pp. 1–21, 2019.
- [41] L. Shang, K. Nienhaus, and G. Nienhaus, “Engineered nanoparticles interacting with cells: size matters,” *Journal of Nanobiotechnology*, vol. 12, no. 1, p. 5, 2014.
- [42] B. Sadeghi, F. S. Garmaroudi, M. Hashemi et al., “Comparison of the anti-bacterial activity on the nanosilver shapes: nanoparticles, nanorods and nanoplates,” *Advanced Powder Technology*, vol. 23, no. 1, pp. 22–26, 2012.
- [43] A. Touhami, M. H. Jericho, and T. J. Beveridge, “Atomic Force microscopy of cell growth and division in *Staphylococcus aureus*,” *Journal of Bacteriology*, vol. 186, no. 11, pp. 3286–3295, 2004.
- [44] E.-Y. Lee, D.-Y. Choi, D.-K. Kim et al., “Gram-positive bacteria produce membrane vesicles: proteomics-based characterization of *Staphylococcus aureus*-derived membrane vesicles,” *Proteomics*, vol. 9, no. 24, pp. 5425–5436, 2009.



Hindawi
Submit your manuscripts at
www.hindawi.com

